Inorg. Chem. **2003**, *42*, 3765–3771

X-ray and Neutron Diffraction Studies on "$Li_{4.4}Sn$"

Corina Lupu, Jiang-Gao Mao, J. Wayne Rabalais, and Arnold M. Guloy*

Department of Chemistry, University of Houston, Houston, Texas 77204

James W. Richardson, Jr.

IPNS Division, Argonne National Laboratories, Illinois 60439

Received December 4, 2002

A chemical analysis and detailed structural characterization, using X-ray single crystal and neutron powder diffraction, of the binary lithium–tin compound "$Li_{4.4}Sn$" is presented. Phase analyses and subsequent structural refinements result in the reformulation of "$Li_{4.4}Sn$" as $Li_{17}Sn_4$. The lithium-rich binary phase crystallizes with a complex cubic structure in the space group $F\bar{4}3m$, with $a = 19.6907(11)$ Å, $Z = 20$. The improved crystal structure determination indicates well-defined lithium atom positions, some of which differ from those previously reported. The nearly Zintl phase $Li_{17}Sn_4$ exhibits poor metallic behavior similar to that of heavily doped semiconductors. Comparisons of the refined crystal structure with previously reported X-ray crystal structures associated with "$Li_{4.4}Sn$" are discussed.

Introduction

Rechargeable solid-state lithium ion batteries have recently come into use as state-of-the-art energy sources for portable commercial electronic devices.[1,2] Lithium ion batteries offer higher energy density than other rechargeable batteries and make them attractive for future electric vehicle applications. Furthermore, Li ion batteries meet the need for compact size, light weight, and high performance for other portable electric applications. Commercial lithium ion batteries currently employ nonaqueous electrolytes, cathodes made with layered lithium cobalt oxide, and carbon anodes. However, the current electrode materials exhibit certain limitations in that only 50% of the theoretical capacity of lithium cobalt oxide can be used and cobalt is relatively expensive and toxic. Moreover, carbon anodes also exhibit large irreversible capacities. Thus the search for new electrode materials is critical to the development of Li batteries with improved performance. The research on potential electrode materials is guided by the need to develop inexpensive and environmentally benign electrode hosts of high energy density and electrochemical capacity.

A fundamental materials problem associated with Li ion batteries is the design of anode materials that can maintain their integrity over many charge/discharge cycles.[3−5] The practical limitations are mainly due to chemical and structural instabilities that occur during the charge and discharge processes. The chemical and structural instabilities could be overcome partly by chemical/surface modification of the electrodes to stabilize the electrode−electrolyte interface, and through chemical substitutions to modulate ion mobility.

Another approach in the development of new anode materials is the use of heterogeneous nanophase materials that exhibit exceptionally high capacities. Thus, extensive studies on a novel tin composite oxide were motivated by its great potential as a viable alternative to carbon-based anodes, with larger capacities (2×) and enhanced safety.[2,6,7] However, a clear understanding of the actual chemical mechanism and structure−property relationships for the much-improved performance of the material is still unsettled. The current opinion about the electrochemical mechanism, supported by indirect evidence, asserts that lithium metal initially reduces tin oxide to metallic tin. The reduction, accompanied by an irreversible formation of amorphous

* To whom correspondence should be addressed. E-mail: aguloy@uh.edu. Phone: +1-713-743-2792. Fax: + 1-713-743-2787.

(1) Poizot, P.; Laruelle S., Grugeon, S.; Dupont, L.; Tarascon, J. M. *Nature* **2000**, *47*, 496−499.
(2) Idota, Y.; Kubota, T.; Matsufuji, A.; Maekawa, Y.; Miyasaka, T. *Science* **1997**, *276*, 1395−1397.
(3) Courtney, I. A.; Dahn, J. R. *J. Electrochem. Soc.* **1997**, *144*(6), 2045−2052.
(4) Mao, O.; Dunlap, R. A.; Dahn, J. R. *J. Electrochem. Soc.* **1999**, *146*(2), 405−413.
(5) Manthiram, A.; Kim, J. *Chem. Mater.* **1998**, *10*, 2895−2909.
(6) Goward, G. R.; Leroux, F.; Power, W. P.; Ouvrard, G.; Dmowski, G.; Egami, T.; Nazar L. F. *Electrochem. Solid-State Lett.* **1999**, *2*(8), 367−370.
(7) Courtney, I. A.; Dahn J. R. *J. Electrochem. Soc.* **1997**, *144*(9), 2943−2948.

10.1021/ic026235o CCC: $25.00
Published on Web 05/21/2003

Li_2O, is then followed by a *reversible* reaction of tin with excess lithium metal that results in the formation of the binary intermetallic compound "$Li_{4.4}Sn$".[3,4]

$$SnO_2 + 4Li \rightarrow 2Li_2O + Sn$$

$$Sn + 4.4Li \leftrightarrow \text{"}Li_{4.4}Sn\text{"}$$

Hence, understanding the facile reversibility of the lithiation−delithiation process is crucial to improved battery performance. It was also suggested that aggregation of tin hinders the reversibility of the lithiation−delithiation process, which leads to a significant decline in anode lifetime and performance.[8] However, key questions concerning structure−property relationships and the kinetics of lithium insertion/extraction − particularly, where and how the ions are located in the host material − are still unresolved. Likewise, although the role of the binary "$Li_{4.4}Sn$" is clearly important to the electrochemical mechanism, the full characterization of the binary phase "$Li_{4.4}Sn$" is still inconclusive. Previously reported X-ray crystal structure investigations on the binary lithium tin phase "$Li_{4.4}Sn$" have so far been inconclusive.[9,10,12,14] The disagreement among the structural reports lies with the actual lithium composition and lithium positions in the lattice. However, obtaining accurate lithium positions and site occupancies from X-ray diffraction is very limited, particularly in the presence of heavy scatterers such as tin. Thus, there is yet no satisfactory resolution regarding the actual lithium composition, crystal structure, bonding description, and properties of "$Li_{4.4}Sn$".

This work reports the chemical composition and structural characterization of "$Li_{4.4}Sn$". In this study the structural characterization involves both X-ray single crystal and neutron powder diffraction analyses and confirms the reassignment of the binary phase "$Li_{4.4}Sn$" as $Li_{17}Sn_4$.

Experimental Section

Synthesis. Handling of all reactants and products was performed within argon-filled gloveboxes (with moisture levels < 0.1 ppm) due to the sensitivity of lithium to nitrogen and the general sensitivity of these materials to air and moisture. The dark gray title compound, $Li_{17}Sn_4$, was obtained in high yield (>95%) by reacting the pure elements: lithium foil (99.9%, Aldrich Chemical) and tin shots (99.999%, Alfa Aesar) (with 12% excess Li), within welded Ta tubes that were sealed under Ar atmosphere. The reaction tubes were placed in evacuated quartz jackets, sealed and heated at ~350 °C for 5 days. The homogeneity (>95%) of the $Li_{17}Sn_4$ samples was established through careful comparison of the experimental X-ray powder diffraction pattern with the calculated diffraction pattern obtained from single-crystal structure refinement. The homogeneity within the grains of the polycrystalline products was also confirmed by scanning electron microscopy (SEM). The observed lattice parameters for $Li_{17}Sn_4$ were essentially constant, over the range of nominal lithium stoichiometry, indicating that the binary title compound exhibited a narrow homogeneity range.

X-ray Crystallography. A shiny dark gray cubic crystal (~0.1 × 0.1 × 0.1 mm) of $Li_{17}Sn_4$ was isolated and sealed within thin-walled glass capillaries under Ar atmosphere. X-ray diffraction data were collected using a Siemens SMART 1K CCD (Mo Kα radiation, graphite monochromator) at 223 K. The cell constants were indexed from 47 reflections chosen from 60 frames collected with 15 s exposure per frame. A hemisphere of data (1271 frames at 5 cm detector distances) was collected by the narrow frame method with scan widths of 0.3° in ω and exposure time of 40 s per frame, $2\theta_{max} = 56.74°$. The first 50 frames were re-collected, after data collection, to monitor the stability of the crystal. The decay in intensity was found to be less than 1.0%. The data were corrected for Lorentz factor, polarization, and air absorption due to variations in the path length through the detector faceplate. The absorption correction was applied by using the PSISCANS program.[15] A total of 12003 reflections were measured, of which 961 reflections were independent, and 732 reflections had $I > 2\sigma_I$ and were used in the structure refinement.

The phase problem was solved by direct methods (SHELXTL). The observed Laue symmetry, systematic absences, and the *E*-statistical values indicated that the possible space groups were $Fd\bar{3}m$ and $Fd\bar{3}$. However, no reasonable solutions could be obtained for these space groups. Related space groups, $F23$ and $F\bar{4}3m$, were used and yielded reasonable solutions. Subsequent structural refinement established the correct space group to be $F\bar{4}3m$.

The full-matrix least-squares refinement resulted in 4 independent Sn positions with well-behaved anisotropic thermal parameters. Subsequently, 13 Li positions were obtained from careful inspection of the Fourier difference maps. Satisfactory isotropic thermal parameters were obtained for 10 Li positions. The thermal parameters for the remaining three Li atoms were assigned ($U = 0.02$) in order for the refinement to converge with satisfactory final residuals ($R = 3.27\%$ and $R_w = 3.82\%$). Due to the low atomic number and weak scattering factor of the lithium atoms, refinement of their anisotropic thermal parameters and occupancies was deemed meaningless. Attempts to refine the structural model using the lower symmetry space group $F23$ did not improve the refinement, and the space group with higher symmetry $F\bar{4}3m$ was chosen. Moreover, the refinement with $F23$ suffered from poor convergence.

The stoichiometry obtained from the X-ray single-crystal refinement was found to be $Li_{340}Sn_{80} = Li_{17}Sn_4$, with all lithium sites fully occupied. This is in good agreement with results of chemical analysis performed on single-phase powder samples (~500 mg) by Galbraith Inc. Results of the bulk chemical analyses indicated a composition corresponding to $Li_{17.05(6)}Sn_{4.00(1)}$, with a carbon content less than 0.1 atom %. Tables 1 and 2 list the relevant crystallographic data and important interatomic distances and angles.

Neutron Powder Diffraction. Time-of-flight neutron powder diffraction measurements were performed using the General Purpose Powder Diffractometer (GPPD) at the Intense Pulsed Neutron Source (IPNS), Argonne National Laboratory. A powder sample (~6 g) of "$Li_{4.4}Sn$", single phase based on X-ray diffraction, was sealed in a 1.6 cm^3 thin-walled vanadium container, with He exchange gas. The sample was then placed on a two-stage displex refrigerator and into the proper sample position. Data collection

(8) Courtney, I. A.; McKinnon, W. R.; Dahn, J. R. *J. Electrochem. Soc.* **1999**, *146*(1), 59−68.
(9) Gladyeshevskii, E. I.; Oleksiv, G. I.; Kripyakevich, P. I. *Sov. Phys.−Crystallogr.* **1964**, *9*(3), 269−271.
(10) Zalkin, A.; Ramsey, W. J. *J. Phys. Chem.* **1958**, *62*, 689−693.
(11) Shimizu, K.; Ishikawa, H.; Takao, D.; Yagi, T.; Amaya, K. *Nature* **2002**, *419*, 597−599. Ashcroft, N. W. *Nature* **2002**, *419*, 569−572.
(12) Nesper, R.; Schnering, H. G. *J. Solid State Chem.* **1987**, *70*, 48−57.
(13) Nesper, R. Dissertation, University of Stuttgart, 1997.
(14) Goward, G. R.; Taylor, N. J.; Souza, D. C. S.; Nazar, L. F. *J. Alloys Compd* **2001**, *329*, 82−91.
(15) SHELXL96: Sheldrick, G., Institut für Anorganische Chemie: Göttingen, Germany, 1996. PSISCANS: North, A. C. T.; Philips, D. C.; Mathews, F. S. *Acta Crystallogr.* **1968**, *A24*, 351−359.

Table 1. Summary of the X-ray Single-Crystal Refinement for $Li_{17}Sn_4$

chem formula	$Li_{17}Sn_4$	fw (g/mol)	592.74
a (Å)	19.6907(11)	space group	$F\bar{4}3m$ (No. 216)
V (Å^3)	7634.6(7)	T (K)	223(2)
Z	20	λ, Mo Kα (Å)	0.71073
		d_{calc} (g/cm^3)	2.578
		μ (mm^{-1})	6.413
		R^a indices ($I > 2\sigma$)	R1 = 0.0327, wR2 = 0.0382

[a] $R1 = \sum||F_o| - |F_c||/\sum|F_o|$; $wR2 = [\sum w(|F_o|^2 - |F_c|^2)^2/\sum w(|F_o|^2)^2]^{1/2}$, $w = 1/(\sigma_F^2)^2$.

times for 295 and 10 K data were 37 and 45 h, respectively. Rietveld profile refinements were carried out using the GSAS program suite using data from the ±145° and ±90° GPPD detector banks, with d spacing ranges of 0.90−2.85 and 0.88−3.99 Å, respectively.[16]

Rietveld powder refinements on $Li_{17}Sn_4$ were carried out on two sets of neutron diffraction data taken at two temperatures (300 and 10 K). The refined structures obtained from previous single crystal investigations were used as initial models for the Rietveld refinements. Final results from the two neutron powder refinements (room temperature and low temperature) indicated a crystal structure with 4 tin and 13 lithium crystallographically independent sites, in agreement with our X-ray single-crystal diffraction results. Refinement of lithium site occupancies indicated negligible deviations from ideal values and supported the results of chemical analyses. The results of the Rietveld refinements are summarized in Tables 3 and 4. The resulting lithium−tin stoichiometry obtained from the Rietveld refinements corresponded to $Li_{340}Sn_{80} = Li_{17}Sn_4$.

The neutron diffraction refinements were hampered by the presence of an unexpected minor secondary phase. However, the secondary phase was not observed in any of the X-ray powder diffraction patterns. The diffraction peaks assigned to the secondary phase were modeled with the LeBail procedure that fits intensities without calculating structure factors. The modeling procedure of the diffraction peaks assigned to the minor phase resulted in a body-centered unit cell with lattice parameter $a \sim 10.96$ Å. Since the LeBail procedure cannot fit intensities, the overlap of reflections due to the primary and secondary phases cannot be determined accurately. Thus, it was necessary to restrict the number of variable parameters in the major $Li_{17}Sn_4$ phase, including the isotropic Debye−Waller factors for identical atoms, e.g., Sn and Li atoms, and fixing the absorption correction coefficients once they were established. Table 3 presents the results of these refinements, and the Rietveld refinement patterns are shown in Figure 1. Structural studies and phase analyses of the secondary minor phase are currently in progress.

Resistivity Measurements. The electronic transport behavior of $Li_{17}Sn_4$ was determined using the electrodeless Q-method on a 70 mg sample that had been sieved to 250−425 μm powder and diluted with chromatographic Al_2O_3.[17,18] The Q-measurements were made at 34 MHz over the temperature range 120−240 K.

Results and Discussion

Using X-ray powder film techniques, "$Li_{4.4}Sn$" was first reported to be analogous to and isostructural with $Li_{22}Pb_5$.[9] This structure type is described as having a large 6 × 6 × 6 superstructure of body centered cubic subcells (216) with $(1/6)a_{super} = a_{subcell}$. The total number of atoms in the unit cell is 432 (each bcc subcell having two atoms: 216 subcells

Table 2. Relevant Interatomic Distances (Å) and Bond Angles (deg) from Refinement of Single-Crystal X-ray Diffraction Data at 223 K and Rietveld Refinement of Neutron Powder Diffraction Data at Both 300 and 10 K

	neutron powder data	
X-ray data	300 K	10 K
	Distances	
Sn(1)−Li(1)(×1) = 2.923(4)	Sn(1)−Li(1)(×1) = 3.193(18)	Sn(1)−Li(1)(×1) = 2.916(22)
Sn(1)−Li(3)(×2) = 2.856(3)	Sn(1)−Li(3)(×2) = 2.623(20)	Sn(1)−Li(3)(×2) = 2.978(12)
Sn(1)−Li(4)(×2) = 2.898(2)	Sn(1)−Li(4)(×2) = 2.950(7)	Sn(1)−Li(4)(×2) = 3.039(9)
Sn(1)−Li(7)(×4) = 3.122(14)	Sn(1)−Li(7)(×4) = 3.116(9)	Sn(1)−Li(7)(×4) = 2.945(6)
Sn(1)−Li(11)(×2) = 3.027(15)	Sn(1)−Li(11)(×2) = 3.076(10)	Sn(1)− Li(11)(×2) = 2.956(12)
Sn(1)−Li(13)(×2) = 3.085(3)	Sn(1)−Li(13)(×2) = 2.937(13)	
Sn(2)−Li(1)(×3) = 2.930(2)	Sn(2)−Li(1)(×3) = 2.751(9)	Sn(2)−Li(1)(×3) = 2.921(13)
Sn(2)−Li(5)(×3) = 2.870(2)	Sn(2)−Li(5)(×3) = 2.841(18)	Sn(2)−Li(5)(×3) = 2.771(13)
Sn(2)−Li(6)(×1) = 2.920(4)	Sn(2)−Li(6)(×1) = 3.277(27)	Sn(2)−Li(6)(×1) = 2.998(23)
Sn(2)−Li(8)(×1) = 2.848(2)	Sn(2)−Li(8)(×1) = 2.894(8)	Sn(2)−Li(8)(×1) = 2.927(7)
Sn(2)−Li(12)(×3) = 3.060(3)	Sn(2)−Li(12)(×3) = 3.142(13)	Sn(2)−Li(12)(×3) = 3.156(13)
Sn(2)−Li(13)(×3) = 2.950(3)	Sn(2)−Li(13)(×3) = 3.306(16)	Sn(2)−Li(13)(×3) = 2.895(12)
Sn(3)−Li(2)(×2) = 2.927(7)	Sn(3)−Li(2)(×2) = 2.943(9)	Sn(3)−Li(2)(×2) = 2.948(5)
Sn(3)−Li(5)(×2) = 2.840(2)	Sn(3)−Li(5)(×2) = 2.854(17)	Sn(3)−Li(5)(×2) = 2.879(14)
Sn(3)−Li(6)(×2) = 2.989(9)	Sn(3)−Li(6)(×2) = 2.898(7)	Sn(3)−Li(6)(×2) = 2.982(5)
Sn(3)−Li(7)(×2) = 2.840(2)	Sn(3)−Li(7)(×2) = 2.874(14)	Sn(3)−Li(7)(×2) = 3.123(11)
Sn(3)−Li(10)(×1) = 2.980(4)	Sn(3)−Li(10)(×1) = 2.703(25)	Sn(3)−Li(10)(×1) = 2.929(19)
Sn(3)−Li(13)(×4) = 3.170(2)	Sn(3)−Li(13)(×4) = 3.114(8)	Sn(3)−Li(13)(×4) = 3.242(9)
Sn(4−Li(3)(×3) = 2.760(3)	Sn(4)−Li(3)(×3) = 2.903(19)	Sn(4)−Li(3)(×3) = 2.777(12)
Sn(4−Li(5)(×3) = 2.990(2)	Sn(4)−Li(5)(×3) = 3.063(18)	Sn(4)−Li(5)(×3) = 3.144(14)
Sn(4−Li(9)(×3) = 2.993(8)	Sn(4)−Li(9)(×3) = 2.988(11)	Sn(4)−Li(9)(×3) = 2.892(9)
Sn(4−Li(10)(×3) = 2.950(2)	Sn(4)−Li(10)(×3) = 3.138(14)	Sn(4− Li(10)(×3) = 2.886(12)
Sn(4)−Li(12)(×1) = 3.028(5)	Sn(4)−Li(12)(×1) = 2.966(25)	Sn(4)−Li(12)(×1) = 3.080(28)
	Angles	
Li(7)−Sn(1)−Sn(1) = 34.61(10)	Li(7)−Sn(1)−Sn(1) = 34.93(15)	Li(7)−Sn(1)− Sn(1) = 31.62(20)
Sn(1)−Li(7)−Sn(1) = 103.7(7)	Sn(1)−Li(7)−Sn(1) = 110.14(40)	Sn(1)−Li(7)−Sn(1) = 116.77(40)
Sn(1)−Li(4)−Sn(1) = 119.75(14)	Sn(1)−Li(4)−Sn(1) = 119.91(60)	Sn(1)−Li(4)−Sn(1) = 111.25(34)
Li(1)−Sn(2)−Li(1) = 105.2(12)	Li(1)−Sn(2)−Li(1) = 104.69(34)	Li(1)−Sn(2)−Li(1) = 109.34(34)
Sn(3)−Li(13)−Sn(3) = 104.85(10)	Sn(3)−Li(13)−Sn(3) = 106.19(5)	Sn(3)−Li(13)−Sn(3) = 103.38(50)
Sn(3)−Li(2)−Sn(3) = 115.66(4)	Sn(3)−Li(2)−Sn(3) = 115.64(31)	Sn(3)−Li(2)−Sn(3) = 118.90(50)
Sn(4)−Li(9)−Sn(4) = 114.47(5)	Sn(4)−Li(9)−Sn(4) = 114.19(34)	Sn(4)−Li(9)−Sn(4) = 111.56(35)
Sn(4)−Li(10)−Sn(4) = 117.29(15)	Sn(4)−Li(10)−Sn(4) = 106.11(70)	Sn(4)−Li(10)−Sn(4) = 111.96(60)

Table 3. Summary of the Rietveld Powder Neutron Refinement for $Li_{17}Sn_4$

bank/phase	parameter	300 K	10K
±145°	*d*-spacing range	0.90−2.85 Å	0.90−2.85 Å
	no. of data points	3921	3921
	no. of reflns ($Li_{17}Sn_4$)	271	271
	no. of reflns (minor phase)	119	125
	R_{wp}	0.0704	0.0930
	R_p	0.0513	0.0621
	R_{F^2}	0.1750	0.1689
±90°	*d*-spacing range	0.88−3.99 Å	0.88−3.99 Å
	no. of data points	2787	2787
	no. of reflns ($Li_{17}Sn_4$)	271	278
	no. of reflns (minor phase)	125	127
	R_{wp}	0.0715	0.0982
	R_p	0.0476	0.0602
	R_{F^2}	0.1579	0.1300
$Li_{17}Sn_4$	space group	$F\bar{4}3m$	$F\bar{4}3m$
	a (Å)	19.7701(2)	19.6680(2)
minor phase	space group	$Im\bar{3}m$	$Im\bar{3}m$
	a (Å)	10.9558	10.9877

Table 4. Relevant Interatomic Distances from Rietveld Neutron Powder Refinements (for 300 and 10 K Data)

300 K	10 K
Sn(2)−Sn(2) = 4.726(13)	Sn(2)−Sn(2) = 4.779(11)
Sn(2)−Li(8) = 2.894(8)	Sn(2)−Li(8) = 2.926(7)
Li(8)−Li(1) = 3.08(15)	Li(8)−Li(1) = 3.371(22)
Li(1)−Li(1) = 4.356(21)	Li(1)−Li(1) = 4.767(30)
Sn(3)−Sn(3) = 4.981(11)	Sn(3)−Sn(3) = 5.087(9)
Sn(3)−Li(13) = 3.114(8)	Sn(3)−Li(13) = 3.242(9)
Li(2)−Li(2) = 2.304(40)	Li(2)−Li(2) = 3.794(31)
Li(6)−Li(2) = 2.335(24)	Li(6)−Li(2) = 2.847(17)
Sn(4)−Sn(4) = 5.017(16)	Sn(4)−Sn(4) = 4.782(12)
Sn(4)−Li(10) = 3.138(14)	Sn(4)−Li(10) = 2.886(12)
Sn(4)−Li(10) = 5.984(23)	Sn(4)−Li(10) = 5.541(20)
Sn(4)−Li(9) = 4.830(27)	Sn(4)−Li(9) = 2.893(9)
Li(10)−Li(10) = 5.175(32)	Li(10)−Li(10) = 4.611(24)
Li(9)−Li(9) = 2.87(4)	Li(9)−Li(9) = 2.998(33)
Sn(1)−Sn(1) = 5.108(11)	Sn(1)−Sn(1) = 5.016(10)
Sn(1)−Li(7) = 3.116(9)	Sn(1)−Li(7) = 2.945(6)
Li(4)−Li(4) = 3.26(5)	Li(4)−Li(4) = 1.839(33)
Li(4)−Li(7) = 4.858(17)	Li(4)−Li(7) = 4.980(22)

× 2 atoms/subcell = 432 atoms).[10] The assigned $Li_{22}Sn_5$ ($Li_{22}Pb_5$ structure type) crystallizes in the space group *F*23 with 4 crystallographically unique Sn atoms (total Sn atoms = 80) located at the following special positions: two Sn at (*x*,*x*,*x*) with $x = -0.0859$ and -0.3359, respectively; one Sn at (*x*,0,0) with $x = 0.3211$; and one Sn at (x,$^1/_4$,$^1/_4$) with $x = 0.0711$. Each bcc subcell contains no more than one Sn atom. The remaining 352 sites in the 6 × 6 × 6 superstructure were assumed to be occupied by lithium. Thus, the resulting structure had the formula $Li_{352}Sn_{80} = Li_{22}Sn_5$. Interestingly, the bcc subcells in $Li_{22}Sn_5$ are analogous with the unit cell of Li metal which was recently found to be a superconductor at high pressures (>30 GPa) with a reported transition temperature (T_C) of ~20 K, the highest T_C for any element.[11]

Progress in understanding the structure of the lithium tin compound "$Li_{4.4}Sn$" was achieved when X-ray single-crystal diffraction investigations by Nesper and von Schnering resulted in the discovery and description of the $Li_{21}Si_5$ structure type.[12] The new structure type, derived from the $Li_{22}Pb_5$-type, was assigned to a higher symmetry space group, $F\bar{4}3m$, a supergroup of *F*23. Furthermore, Nesper and von Schnering proposed the reassignment of isotypical compounds in the $Li_{22}Pb_5$ family, including "$Li_{4.4}Sn$", to the $Li_{21}Si_5$ structure type. Thus, "$Li_{4.4}Sn$" was consequently reformulated as $Li_{21}Sn_5$.[13]

The crystal structure of $Li_{21}Sn_5$ ($Li_{21}Si_5$ structure type) can be derived from the complex bcc structure of $Li_{22}Sn_5$ ($Li_{22}Pb_5$ type) but with some structural differences. Of the 432 lattice sites (216 subcells × 2 atoms/subcell) generated in the bcc-derived $Li_{22}Sn_5$ structure, only 80 tin positions and 336 lithium positions were occupied. Thus, 16 Li sites, previously assigned in $Li_{22}Sn_5$, were vacant in $Li_{21}Sn_5$, and this leads to the reformulation of "$Li_{4.4}Sn$" as $Li_{336}Sn_{80} = Li_{21}Sn_5$. The unoccupied lithium sites in $Li_{22}Sn_5$ correspond to centers of nominal M_{26} (M = $Li_{22}Si_4$, $Li_{20}Si_6$) clusters in $Li_{21}Sn_5$. Although modest electron densities were observed at some of the centers of the M_{26} clusters, the occupancies were neglected by Nesper due to unreasonably short interatomic distances.[13]

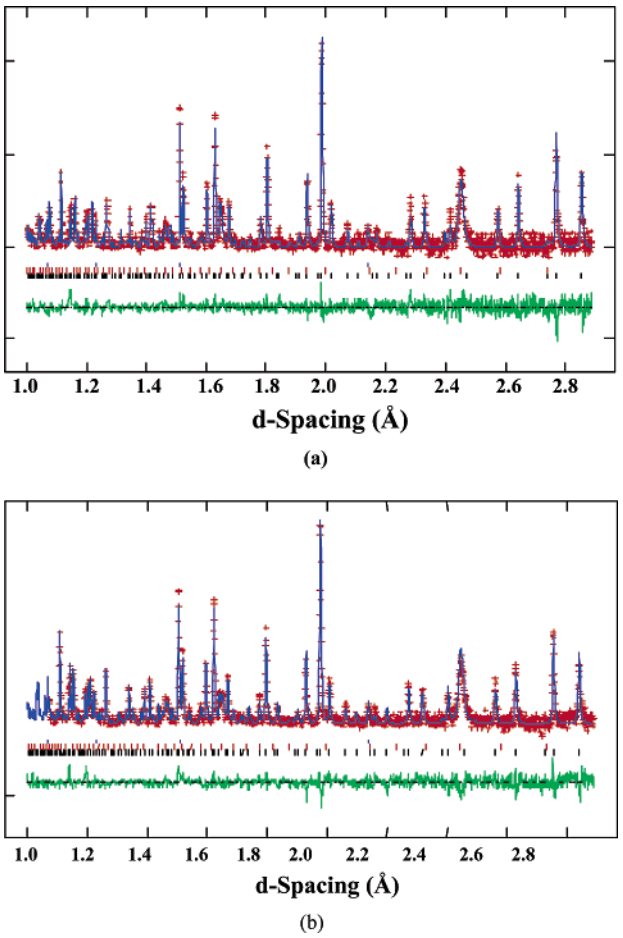

Figure 1. Rietveld profile plots for neutron refinements at (a) 295K and (b) 10 K. The small plus (+) signs represent observed data, the overlaid solid curve is the calculated pattern, and the curve at the bottom of the figure is a difference plot, i.e., (observed − calculated). All data are presented with the background subtracted and with spectra normalized to the GPPD incident spectrum. The bottom row of vertical bars in the middle of the figure represents locations for reflections in the $Li_{17}Sn_4$, while the middle and the top rows represent reflections in the impurity phase and vanadium (from the container).

(16) Larson, A. C.; Von Dreele, R. B. Los Alamos National Laboratory Report No. LA-UR-86-748, 1987.
(17) El-Hanany, U. *Rev. Sci. Instrum.* **1973**, 44(8), 1067−1068.
(18) Shinar, J.; Dehner, B.; Beaundry, B. J.; Peterson, D. T. *Phys. Rev. B* **1988**, *37*(4), 2066−2073.

Recently, Nazar and co-workers[14] reported single-crystal X-ray diffraction studies on the family of lithium tetrelides, $Li_{21}X_5$ (X = Si, Ge, Sn, and Pb). Their reinvestigation of $Li_{21}Sn_5$ indicated that the actual stoichiometry, based on X-ray structure refinement, is $Li_{21.31}Sn_5$. Consequently, $Li_{21}Sn_5$ was reformulated as a nonstoichiometric phase $Li_{17.05}Sn_4$. Many of the differences between the Nesper[13] and Nazar[14] structures are based on some lithium positions and their occupancies. Some of the minor residual densities previously ignored by Nesper,[13] due to unreasonable Li interatomic distances, were later refined as partially occupied Li sites by Nazar.[14] The partially occupied Li sites were subsequently described as representing crystallographic disorder over the relevant Li sites. Nevertheless, the use of conventional X-ray diffraction experiments to obtain accurate partial site occupancies of weak X-ray scatterers such as Li is suspect, particularly in the presence of heavy scatterers such as Sn.

Our structural investigations, involving the use of both X-ray single-crystal and neutron powder diffraction, resulted in a stoichiometric binary phase $Li_{17}Sn_4$. The atomic positions for Sn atoms were determined by X-ray single-crystal diffraction and confirmed by the results of the Rietveld refinement. Since lithium atoms scatter neutrons better than tin atoms, the neutron diffraction results provided a more accurate description of the lithium sites and occupancies. The refinement of both X-ray and neutron diffraction data resulted in very similar crystal structures. In particular, the room temperature neutron diffraction data and the single-crystal X-ray refinement yielded almost identical results.

To understand the resulting complex cubic structure we will reduce and describe the crystal structure in terms of four different geometrical building units of M_mX_x (M = tin; X = lithium) clusters. There are two octahedral M_6X_{20} units (***A*** and ***B***) containing two interpenetrating tetrahedral Li "clusters" (Li_8) enclosed within an octahedral Sn_6 arrangement. The remaining 12 Li atoms in each M_6X_{20} unit bridge the edges of the Sn_6 octahedra. The differences between ***A*** and ***B*** lie in the placement of the enclosed Li_8 unit of two interpenetrating tetrahedra. The two nominal octahedral building units, ***A*** and ***B***, are illustrated in Figure 2a. A third building unit is an M_4X_{23} arrangement (***C***) that features a Li-centered Sn_4 tetrahedral core. The remaining lithium atoms of the M_4X_{23} unit are arranged as face-capping (4×), edge-bridging (6×), and terminal (12×) ligands around the $LiSn_4$ core. The fourth building unit, a tetrahedral M_4X_{22} arrangement (***D***), is similar to ***C*** but with centers of the Sn_4 tetrahedra empty. Due to the vacancy at the centers of ***D***, the face-capping lithium atoms seemingly collapse toward the center and nearly lie on the faces of the Sn_4 units. The tetrahedral building units ***C*** and ***D*** are shown in Figure 2b. The nominal tin "cluster" arrangements in ***A***, ***B***, ***C***, and ***D*** are mere geometrical units, and no chemical bonds are assumed between Sn atoms (the nearest Sn−Sn distances being greater than 4.659 Å).

The centers of the nominal M_6X_{20} octahedral arrangements, as well as the tetrahedral M_4X_{23} and M_4X_{22} arrangements (***A***, ***B***, ***C*** and ***D***, respectively), are located along (0,0, *z*), (0,½, *z*), and (½,½, *z*). Each of the nominal clusters forms closed packed layers perpendicular to the body diagonal of the cubic cell, and the layers are stacked with the sequence ***CDABC′D′A′B′***. The packing arrangements of the nominal clusters are shown in Figure 3, with the lithium atoms removed for simplicity. The resulting complex crystal structure, as shown in Figure 4, features the bridging lithium atoms of the nominal clusters interpenetrating and linking with neighboring clusters.

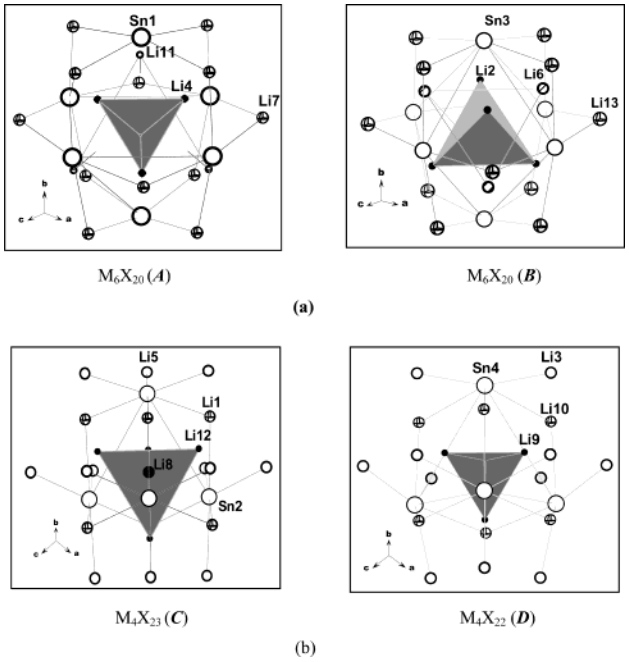

Figure 2. (a) Octahedral M_6X_{20} (***A***) and M_6X_{20} (***B***) arrangements. (b) Tetrahedral M_4X_{23} (***C***) and M_4X_{22} (***D***) arrangements. The Sn, bridging Li atoms, and the terminal Li atoms are represented as large open circles, small octands, and small open circles, respectively.

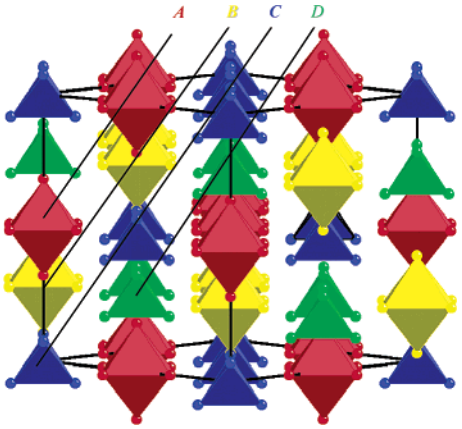

Figure 3. Representation of the stacking of closed-packed layers formed by ***A*** (red), ***B*** (yellow), ***C*** (blue), and ***D*** (green). The layers lie perpendicular to the body diagonal of the cubic cell, with a repeat stacking sequence ***CDABC′D′A′B′***.

The structure of $Li_{17}Sn_4$, as described in this paper, is similar to the $Li_{21}Sn_5$ structure of Nesper.[13] A direct symmetry correspondence is observed between all tin and lithium positions found by Nesper and those described herein. However, the difference between the two crystal structures lies with an additional Li site (Li6), which completes the coordination sphere around the Sn2 site, in $Li_{17}Sn_4$. The site

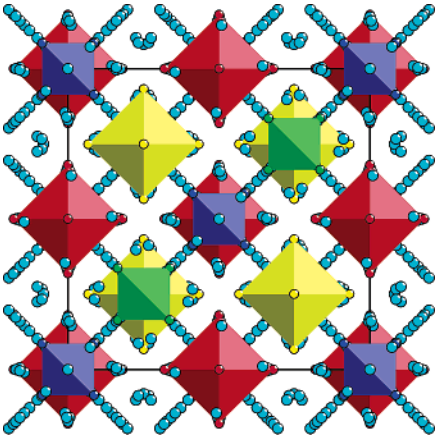

Figure 4. Polyhedral representation of the $Li_{17}Sn_4$ crystal structure. The different Sn octahedral and tetrahedral arrangements are represented as colored polyhedra ***A*** (red), ***B*** (yellow), ***C*** (blue), and ***D*** (green). Lithium atoms are represented as cyan-colored spheres.

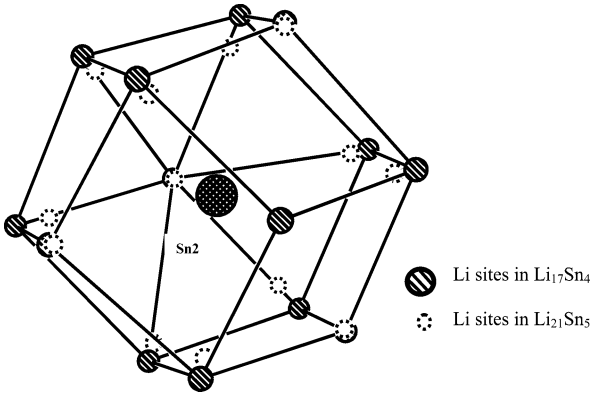

Figure 5. A schematic representation of the differences in the coordination environment, around Sn2, in $Li_{17}Sn_4$ and $Li_{21}Sn_5$ ($Li_{21}Si_5$ type).

also corresponds to the lithium atom located at the center of the M_4X_{23} unit ***C***. The sites were previously ignored during the refinement of the $Li_{21}Si_5$ structure type due to unreasonable lithium distances.[12] However, results of our structure refinements indicate reasonable lithium distances (2.8−2.9 Å) corresponding to these sites. The differences in the pertinent lithium positions around the Sn2 site in $Li_{17}Sn_4$ and $Li_{21}Sn_5$ are illustrated in Figure 5. Results of our X-ray single crystal and powder neutron diffraction studies do not agree with some lithium sites reported by Nazar, particularly those that were reported as having partial occupancies.[14]

A comparison of the occupancies of relevant sites at special positions 4a, 4b, 4c, and 4d summarizes the main differences between the reported crystal structures associated with "$Li_{4.4}Sn$". These lattice sites represent the centers of each nominal cluster arrangement ***A***, ***B***, ***C***, and ***D***. A summary of the lithium occupancies at these sites, based on the different structural studies, is presented in Figure 6. In $Li_{22}Sn_5$ ($Li_{22}Pb_5$ type) all of the relevant sites, 4a, 4b, 4c, and 4d, were assumed to be occupied by lithium atoms.[10] In $Li_{21}Sn_5$ ($Li_{21}Si_5$ type), all of the 4a, 4b, 4c, 4d sites were ignored and considered vacant due to the unreasonable interatomic distances that resulted from lithium occupancy of these sites.[13] Our $Li_{17}Sn_4$ model, as described in this report, indicate Li occupancies only at the 4a sites, which corresponds to the center of the nominal M_4X_{23} cluster. In the previously published $Li_{17}Sn_4$ structure, partial and full occupancies by Li atoms on the 4c (25% occupancy) and 4d (100% occupancy) sites were reported.[14] Furthermore, the

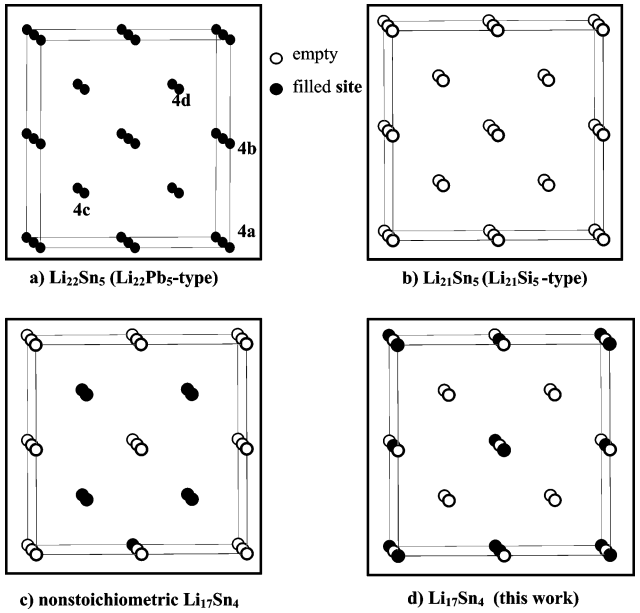

Figure 6. An illustrative summary of the lithium occupancies of the 4a, 4b, 4c, 4d special positions in (a) $Li_{22}Sn_5$ ($Li_{22}Pb_5$ type); (b) $Li_{21}Sn_5$ ($Li_{21}Si_5$ type); (c) nonstoichiometric $Li_{17}Sn_4$ model; and (d) $Li_{17}Sn_4$ (this work).

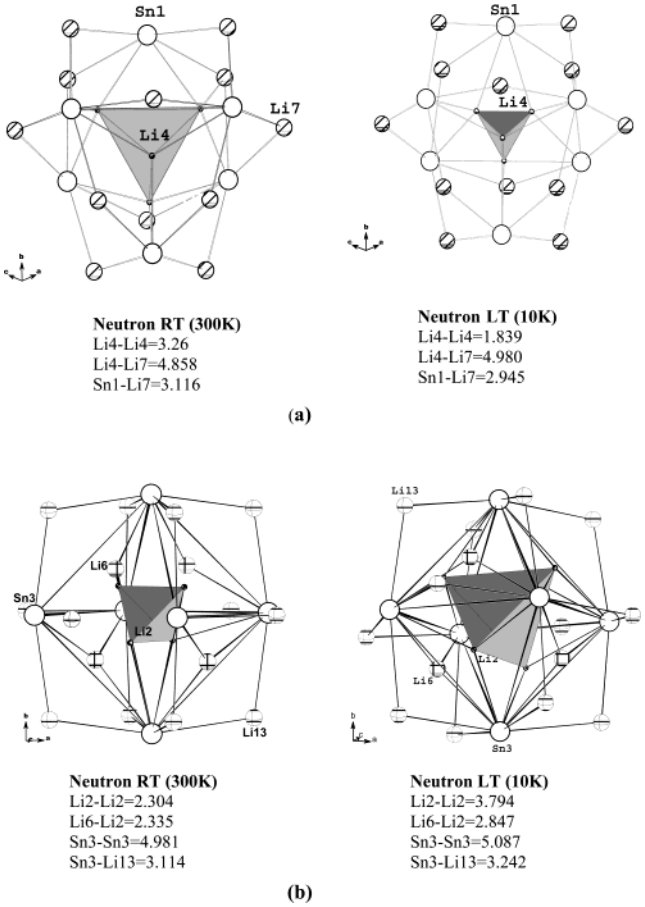

Figure 7. An illustrative comparison of the Li atom positions from results of Rietveld neutron refinements at 300 and 10 K for (a) the M_6X_{20} (***A***) "cluster" and (b) the M_6X_{20} (***B***) "cluster".

previously reported nonstoichiometric model also featured partial occupancies at two other lithium sites 16e with 75% and 25% occupancies.[14] Attempts to refine X-ray single-crystal data using the nonstoichiometric $Li_{17}Sn_4$ model were unsuccessful in locating the problematic Li sites. Likewise, Rietveld profile refinements on the neutron powder data, using positional parameters from the nonstoichiometric $Li_{17}Sn_4$ model, were also unsuccessful.

Additional observations can be made regarding the neutron powder diffraction results obtained at 300 and 10 K. The lattice parameters obtained from neutron diffraction experiments performed at 300 and 10 K are 19.7701(2) and 19.6680(2) Å, respectively. The change in unit cell dimension from 300 to 10 K corresponds to a decrease in the unit cell volume, $\Delta V = -1.54\%$. The volume contraction is manifested by atomic displacements upon decreasing the temperature from 300 to 10 K. All Sn atoms remain approximately at the same locations, except for the Sn atoms in ***D*** (M_4X_{22}). The nearest Sn−Sn distances in the "empty" Sn_4 tetrahedral "clusters" decreases from 5.016 Å (300 K) to 4.784 Å (10 K). This confirms the vacancy at the center of the tetrahedral Sn arrangement in ***D***. Among the 13 crystallographically unique Li sites, substantial changes in the Li interatomic distances were observed for four lithium sites, as listed in Table 4. Lithium displacements were mainly observed with the enclosed interpenetrating tetrahedral Li_8 arrangements found within ***A*** and ***B*** (M_6X_{20}). The different lithium tin arrangements resulting from the room temperature and low-temperature neutron diffraction data are illustrated in Figure 7. Although there were no changes in symmetry, we may speculate that all the atomic displacements are associated with a displacive phase transition that occurs between 300 and 10 K.

One of the motivations in investigating the crystal structure of the title compound was to understand the chemical bonding of polar intermetallics on the border of being Zintl phases. A simplistic Zintl picture of the bonding in $Li_{17}Sn_4$ is being an electron-rich metallic phase [i.e., $17Li^+ - (4Sn^{4-}) = 1e^-$], the "excess" electron being delocalized in a conduction band. Previous semiempirical band structure calculations (CNDO) performed on $Li_{21}Si_5$ have indicated that the excess electrons in these Li-rich phases are involved in localized lithium cagelike bonding states at the Fermi level.[12] Our calculations (EHMO) on $Li_{17}Sn_4$ yield very similar results. Transport measurements were performed on the single phase samples of $Li_{17}Sn_4$ using the electrodeless Q-method.[16,17] The results of the Q-measurements indicate a small (positive) temperature dependence of the resistivity and suggest that the nearly Zintl phase $Li_{17}Sn_4$ exhibits poor metallic behavior similar to that of heavily doped semiconductors. This is consistent with the electronic description that features weakly delocalized cagelike filled states derived from Li cluster orbitals.

Our reinvestigation of "$Li_{4.4}Sn$" poses questions regarding the role of the binary alloy in the electrochemistry of the tin composite oxide. In a series of electrochemical studies, reports on the presence of $Li_{17}Sn_4$ were based on powder X-ray diffraction patterns of inhomogeneous samples. Moreover, only two diffraction peaks, (110) and (211), were indexed with the cubic cell of $Li_{17}Sn_4$. The severe sensitivity of $Li_{17}Sn_4$ to air and moisture, as evidenced by the immediate formation of gray/white powders upon exposure to air, further poses questions about the stability of $Li_{17}Sn_4$ within the electrochemical cells. However, the possibility of interstitial stabilization of a related ternary cannot be discounted and is quite favored. Studies on the stabilization of pseudo-binary $Li_{17}Sn_4Z_x$ by small interstitial atoms (Z = C, O, N, B) are currently in progress.

Acknowledgment. The authors would like to thank Dr. Jim Korp and Dr. Craig Downie for help with the crystallography and Prof. J. D. Corbett for providing the Q-measurements. Support for this work was provided by the National Science Foundation (CHEM-998607 and DMR-9632667), NSF CAREER Award (DMR-9733587), the ACS-Petroleum Research Fund, Texas Advanced Research Program (Award No. 003652-0002-2001), the U.S. Department of Energy, BES-Materials Science, under Contract W-31-109-Eng-38, and the R. A. Welch Foundation.

Supporting Information Available: Crystallographic data in CIF format. This material is available free of charge via the Internet at http://pubs.acs.org.

IC026235O